Bulletin of the Seismological Society of America, Vol. 98, No. 5, pp. 2118–2132, October 2008, doi: 10.1785/0120070243

A Search for Temporal Variations in Station Terms in Southern California from 1984 to 2002

by Guoqing Lin,* Peter M. Shearer, and Egill Hauksson

Abstract We use relative arrival times and locations for similar earthquake pairs that are found using a cross-correlation method to analyze the time dependence of *P* and *S* station terms in southern California from 1984 to 2002. We examine 494 similar event clusters recorded by Southern California Seismic Network (SCSN) stations and compute absolute arrival-time variations from the differential arrival-time residuals obtained following event relocation. We compute station terms from the robust means of the absolute arrival-time residuals from all events recorded by each station at 3-month intervals. We observe nine stations with abrupt offsets in timing of 20–70 msec, which are likely caused by equipment changes during our study period. Taking these changes into account could improve the relative location accuracy for some of the event clusters. For other stations, we generally do not see systematic temporal variations greater than about 10 msec. Analysis of residuals along individual ray paths does not reveal any clear localized regions of apparent velocity changes at depth. These results limit large-scale, long-lasting temporal variations in *P* and *S* velocities across southern California during this time period to less than about $\pm 0.2\%$. However, there is an increased fraction of individual travel-time residuals exceeding 20 msec immediately following major earthquakes from source regions near the mainshock rupture.

Introduction

Recently, waveform cross correlation has become an increasingly important tool for improving relative earthquake locations, characterizing event similarity, and studying earthquake source properties (e.g., Nakamura, 1978; Poupinet *et al.*, 1984; Got *et al.*, 1994; Dodge *et al.*, 1995; Nadeau *et al.*, 1995; Gillard *et al.*, 1996; Shearer, 1997, 1998; Rubin *et al.*, 1999; Waldhauser *et al.*, 1999; Astiz and Shearer, 2000; Astiz *et al.*, 2000; Shearer, 2002; Shearer *et al.*, 2003; Rowe *et al.*, 2004; Hauksson and Shearer, 2005; Schaff and Waldhauser, 2005; Shearer *et al.*, 2005; Lin and Shearer, 2007; Lin *et al.*, 2007). Relative locations can be greatly improved compared to standard methods because the differential times for events within similar event clusters are much more precise than individual arrival-time picks, and differential location methods can largely remove the biasing effects of a large-scale 3D velocity structure between the source and receiver. Most of these methods implicitly assume stability of seismic velocities and the relative timing among the stations within the recording network. However, it is also possible to use waveform cross-correlation data to search for time dependence in observed travel times, and a number of studies have used this approach to identify (or place limits on) small crustal velocity changes or changes in scattering behavior associated with large earthquakes (e.g., Poupinet *et al.*, 1984; Ellsworth *et al.*, 1987, 1992; Haase *et al.*, 1995; Dodge and Beroza, 1997; Baisch and Bokelmann, 2001; Nakamura *et al.*, 2002; Rubinstein and Beroza, 2004; Peng and Ben-Zion, 2006; Sawazaki *et al.*, 2006; Li *et al.*, 2007). In addition, Rubin (2002) demonstrated that differential times provide precise calibration information for detecting station and network timing discrepancies. He observed abrupt changes in station timing of up to 20 msec, which are associated with changes in station electronics, and found that correcting for these effects can reduce the scatter within clusters of repeating earthquakes and the apparent seismogenic thickness of faults in northern California.

Here, we perform a comprehensive search for possible temporal variations in station timing or seismic velocities across southern California from 1984 to 2002, using relative arrival times and locations from similar event clusters identified in our recent comprehensive relocation of southern California seismicity using waveform cross correlation (Shearer *et al.*, 2005; Lin *et al.*, 2007). We observe nine stations with abrupt offsets in timing of 20–70 msec, which are likely

*Present address: Department of Geology and Geophysics, University of Wisconsin-Madison, Madison, Wisconsin 53706.

caused by equipment changes during our study period. For other stations, we generally do not see systematic temporal variations greater than about 10 msec, although there is an increased fraction of individual travel-time residuals exceeding 20 msec immediately following major earthquakes from source regions near the mainshock rupture.

Method

Our differential times and earthquake locations are from the waveform cross-correlation projects of Shearer *et al.* (2005) and Lin *et al.* (2007), in which events are relocated separately within individual similar event clusters. The similar event clusters are obtained by first searching for correlated event pairs that have eight or more *P* or *S* measurements with correlation coefficients above 0.65 for stations within 80 km of the events. A cluster analysis method is then applied to the set of correlated event pairs to identify robust distinct sets of linked events. These similar event clusters are typically between 1 and 2 km in size and contain from 40 to 1000 events. The relocations are performed assuming that seismic velocities and station timing are constant during the entire 1984–2002 period. Our goal here is to look for possible time dependence in the residuals from the relocations that would suggest some changes in velocity and/or timing have occurred. However, the problem is complicated by the fact that the precise times provided by waveform cross correlation are differential times between a pair of events occurring at different times. Thus, our first step is to estimate absolute time residuals for each event from the set of differential time residuals.

For a similar event cluster with n events recorded by a given station, we may express the differential arrival-time residuals, dr_{ij}, for a pair of events, i and j, after relocation as

$$dr_{ij} = dT^o_{ij} - (dT^p_{ij} + dt_{0ij}) \tag{1a}$$

$$= (T^o_i - T^o_j) - (T^p_i - T^p_j) - (t_{0i} - t_{0j}) \tag{1b}$$

$$= (T^o_i - T^p_i - t_{0i}) - (T^o_j - T^p_j - t_{0j}) \tag{1c}$$

$$= r_i - r_j, \tag{1d}$$

where dT^o_{ij} is the observed differential arrival time between event i and event j measured using waveform cross correlation; dT^p_{ij} is the predicted differential travel time, given the computed event locations and a reference 1D velocity model; and dt_{0ij} is the differential origin time between the two events. The differential times can be written as the differences of the absolute times as in equation (1b) and (1c) so that we can consider the differential arrival-time residual as the difference between the two absolute arrival-time residuals, r_i and r_j, as in equation (1d).

Within each similar event cluster, we apply the Lin *et al.* (2007) method to adjust the event locations and origin times, so as to minimize the differential residuals, dr_{ij}, with respect to a robust misfit measure (a hybrid $l_1 - l_2$ norm that is insensitive to extreme values). These residuals are the starting point for our search for possible time-dependent effects. For each station and similar event cluster, we find the set of values r_k $(k = 1, \ldots, n)$ that best fit the differential values $dr_{ij} = r_i - r_j$. This process is done for each station and phase (P or S) separately, and the values r_k are estimates of the observed timing misfit for each event in the cluster. This problem can be expressed by the following equation for a cluster with n events and N differential time observations:

$$\begin{bmatrix} dr_{12} \\ dr_{13} \\ . \\ dr_{23} \\ . \\ dr_{pq} \end{bmatrix} = \begin{bmatrix} 1 & -1 & 0 & . & . & & . & 0 \\ 1 & 0 & -1 & 0 & . & & . & 0 \\ . & & . & & . & & & . \\ 0 & 1 & -1 & 0 & & . & . & 0 \\ . & & . & & . & & & . \\ 0 & . & 1 & . & . & -1 & . & 0 \end{bmatrix} \begin{bmatrix} r_1 \\ r_2 \\ r_3 \\ . \\ r_n \end{bmatrix}$$

$$= \mathbf{B} \begin{bmatrix} r_1 \\ r_2 \\ r_3 \\ . \\ r_n \end{bmatrix}, \tag{2}$$

where $p, q \in [1, 2, \ldots, n]$ and $\mathbf{B}$ is an $N \times n$ matrix with components only of 1, −1, and 0. We use an iterative method based on the same robust least-squares misfit norm applied in the relocation process. Note that the solution to this problem is not unique, because a constant can be added to each r_k without changing the differential time residuals. We remove this ambiguity by requiring that the solution have zero mean over all r_k $(k = 1, \ldots, n)$. We will show later that this constraint does not affect our results. Because the individual r_k values can exhibit considerable scatter and a longer period would smooth out the temporal variations in shorter time windows, we evaluate the station terms by grouping the events into 3-month periods from 1984 to 2002 for each station and compute the robust mean of r_k within each interval.

Ideally, if a given station recorded the events in a single cluster continuously during our analysis period, this cluster alone could be used to estimate the time-dependent station term for this station. Unfortunately, most of our observed similar event clusters were not continuously active during the entire 1984–2002 time period. Thus, we must combine results from many different similar event clusters to obtain a continuous measure of the station terms. Because we use differential time residuals to estimate demeaned absolute time variations for each cluster, we cannot directly combine the r_k estimates from different clusters. Instead, we compute the best-fitting station terms for the whole period from the

arrival-time variations in different clusters that cover different time periods. The cartoons in Figure 1 show how we are able to recover a continuous trace from the overlapping results from different clusters. In Figure 1, the receiver, shown by the triangle, has a true time variation, r_k $(k = 1, \ldots, n)$, shown by the solid curve in the small panel on the left-hand side of the station, which in this case has nonzero mean. As shown in the right-hand panels, we have demeaned arrival-time variation estimates from four similar event clusters spanning different time periods, which can be expressed as r'_{lp} (where $l = 1$, 2, 3, and 4 representing each cluster and $p \in$ a subset of $[1, \ldots, n]$). From these time series, we solve for an estimate of the complete time series, r'_k, together with individual offset terms for each trace, C_l, that provides the best fit between r'_k and $r_{lp} + C_l$ for each cluster. To obtain a unique solution, we also require that the complete time series estimate have zero mean, that is, that $E(r'_k) = 0$. The dashed curve in the left-hand panel of Figure 1 shows the result of this inversion. Note that even when there is a gap in a particular cluster (e.g., cluster 4 in Fig. 1), the trace is still recovered as long as the gap is filled in from other clusters (cluster 2 in this example). Each recovered subtrace is shifted from its true values, but the relative variations are exactly the same as in the true values. Because we are interested only in the relative variations in station terms, this does not affect our results in this study.

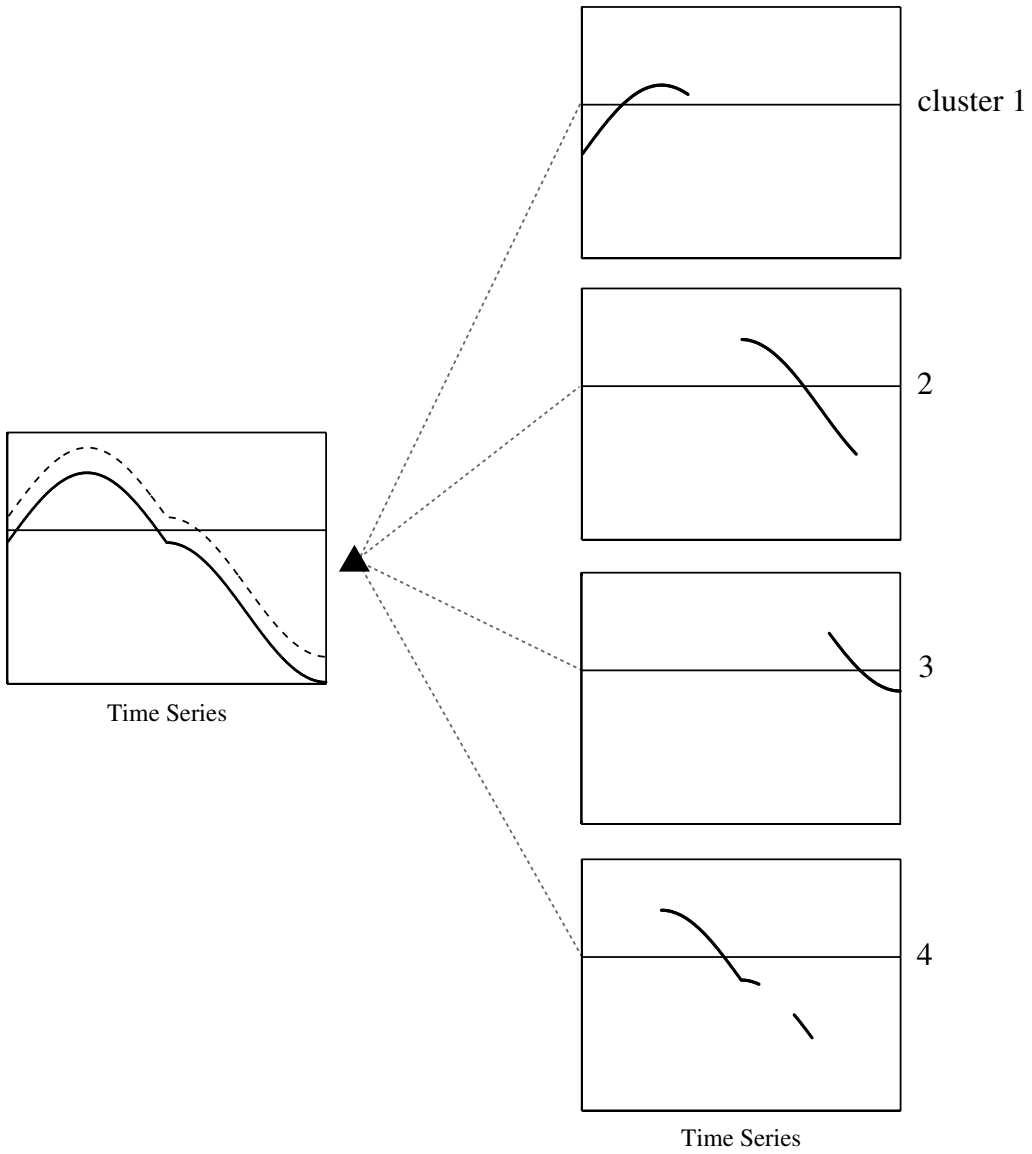

Figure 1. A cartoon showing how a continuous time series, shown by the solid curve on the left-hand side, can be recovered from subtraces, each of which covers only part of it. The triangle in the middle of the figure is the station that records similar event clusters. The subtraces represent the absolute time changes for the events in each cluster in this study. The horizontal lines mark zeros of the absolute values. After we apply our algorithm, the recovered trace, which has zero mean over all the points, is shown by the dashed curve next to the true trace.

After we recover the time variations for the whole recording period, we estimate time-dependent station terms by computing the robust mean of variations from events in 3-month intervals. Note that here we assume that time variations are occurring only at the station and that each subtrace has exactly the same relative variations as in the main trace. If points in some of the subtraces are biased, for example, by temporal variations in seismic velocity along a specific source–receiver path, the recovered main trace will also be biased. However, by including many different similar event clusters for each station, these possible biasing effects will tend to average out. Later, once we have accounted for as much of the differential time residuals with time-varying station terms alone, we will search for possible changes in seismic properties along specific ray paths (see the section Temporal Seismic Velocity Variations?).

Synthetic Data Tests

In order to examine the validity and resolution of our method, we first apply our technique to synthetic data. We randomly selected the station CILAQ from the Southern California Seismic Network (SCSN) station list, where CI is the network code and LAQ is the station name. Figure 2 shows the location of this station as a triangle and its recorded 169 clusters as circles with sizes proportional to the number of events in each cluster.

Based on our experience, we adopted the criteria for both the synthetic and real data that each event pair must have eight or more *P* or *S* measurements with correlation coefficients above 0.65 for stations within 80 km of the events. First, we compute the absolute arrival-time variation for each event in each event cluster after relocation and combine them together for the whole study period using our trace-recovery algorithm. We then group the arrival-time changes from events every 3 months between 1984 and 2002 and calculate the robust mean of these variations as the station correction for each interval. In order to obtain robust estimates, we require that each event have at least five differential times for *P* or *S* variations, respectively, and that each 3-month interval include more than 10 events for the robust mean calculation. The resulting station corrections are shown by the filled circles in Figure 3.

To generate our synthetic data, we added a 25 msec perturbation to the arrival times of events in 1994 and 1995 before relocating the events. By doing this, we assume the station timing was disturbed by 25 msec during this period. The goal of this test is to check how well we can recover this 25 msec perturbation, given that it may bias our computed event locations. After we repeat the same processing steps as for the unperturbed data, we obtain new station corrections

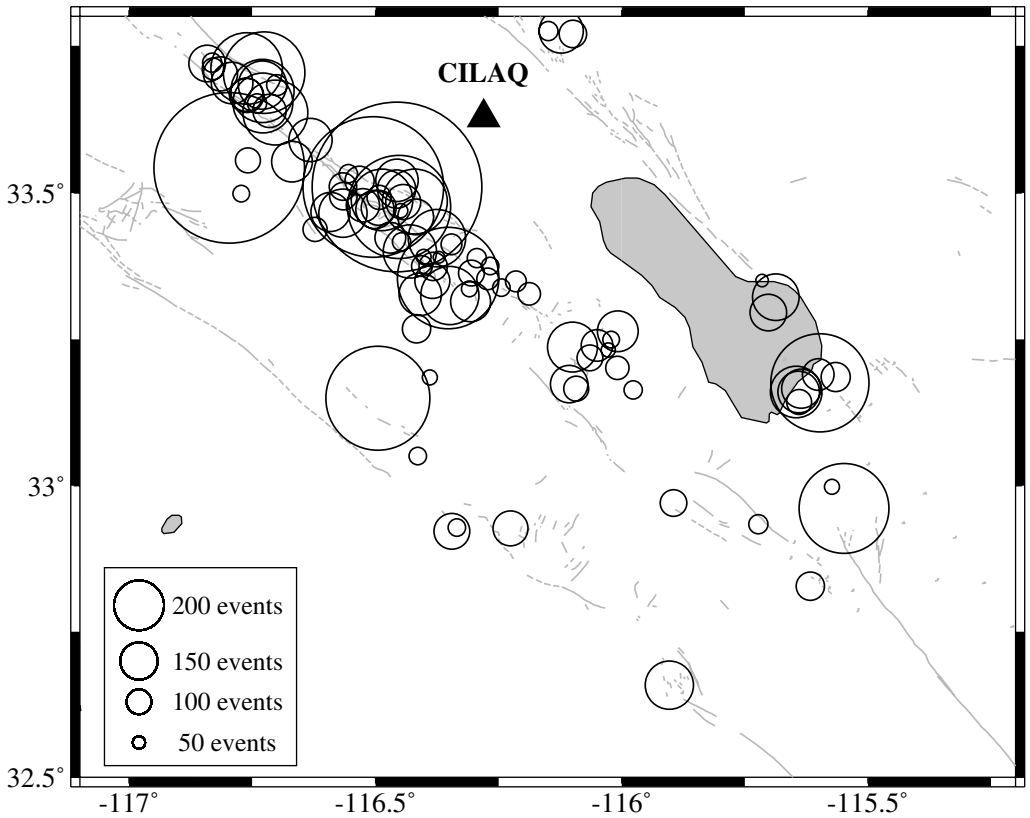

Figure 2. The station CILAQ (triangle) and its recorded 169 similar event clusters (circles) used for a synthetic data test described in the text. Circle diameter is proportional to the number of events in each cluster.

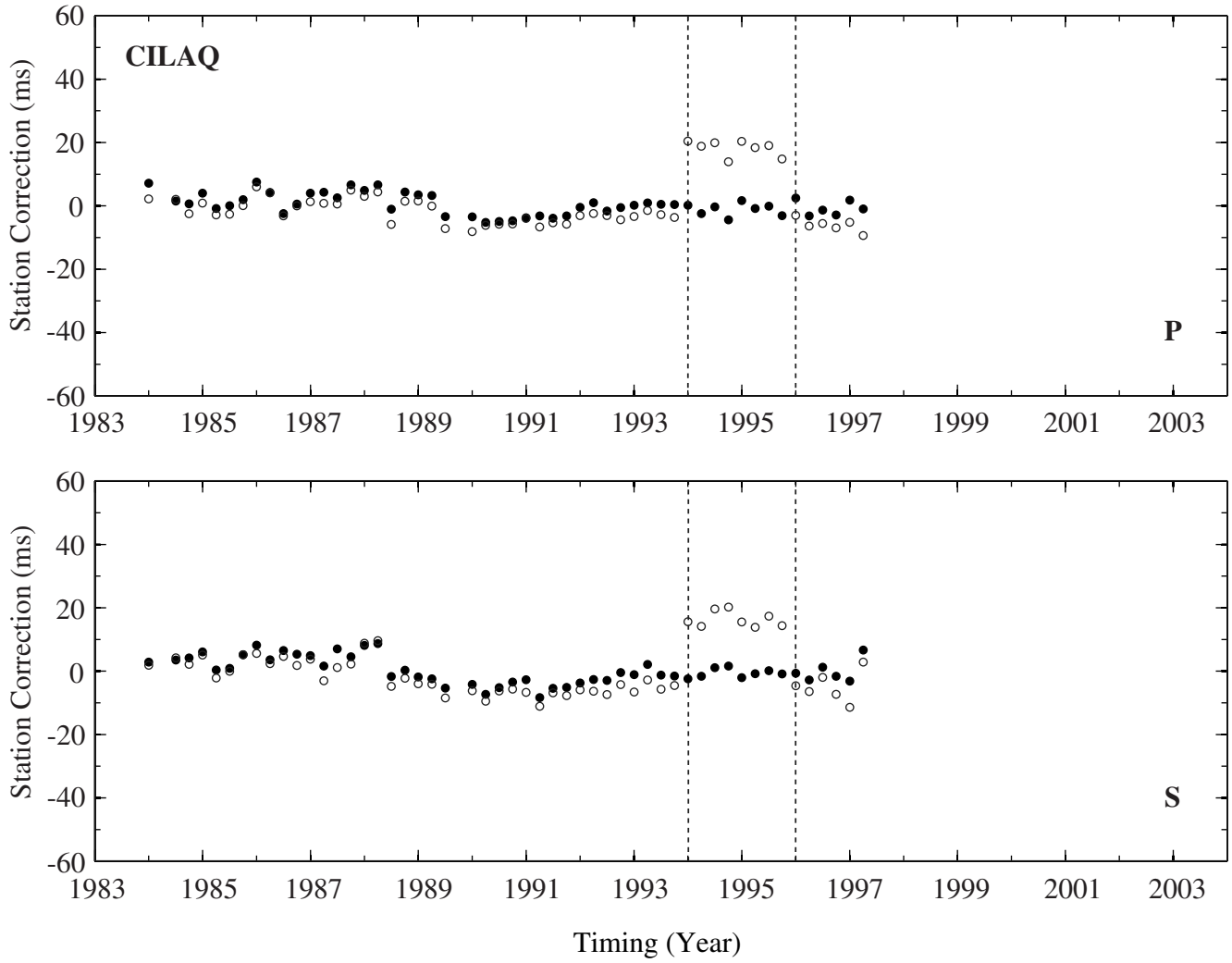

Figure 3. Station corrections for the synthetic data test for station CILAQ for *P* (top) and *S* (bottom). The filled circles represent the actual unperturbed data values, and the open circles are the recovered values after perturbing the travel times for events in 1994 and 1995 by 25 msec.

for CILAQ, which are shown by the open circles in Figure 3. It is clear that the perturbed arrival times in 1994 and 1995 are well resolved. The differences between the perturbed values and the true ones are about 20 msec for *P* and 19 msec for *S*. Because the corrections in other periods are shifted by about 3 msec in the opposite direction, the recovered *P* and *S* perturbations are actually about 23 and 22 msec, respectively. The values in unperturbed periods are altered because (1) the perturbations are added before the differential time relocation and the resulting locations may be slightly different, and (2) the whole time series is required to have zero mean. The values in 1994 and 1995 are shifted by a large amount in the positive direction and thus the other values are moved slightly in the negative direction. We experimented with adding different arrival-time perturbations ranging from 1 to 100 msec and found that the resolution of our technique under ideal conditions is about 2 or 3 msec. Of course, the results would worsen if multiple stations experienced timing offsets so that the computed locations were more severely affected. However, as we will show later, relatively few of the SCSN stations have observable timing changes.

Southern California Data

We selected 494 similar event clusters between 1984 and 2002 from the SHLK location catalog (Shearer *et al.*, 2005) recorded by 166 SCSN stations. All these clusters consist of more than 40 events occurring in different time periods. The cluster locations are shown by the circles in Figure 4, and the stations are shown by the triangles. The filled triangles are the nine stations for which we find significant arrival-time variations in our study (see the following discussion). The stars show epicenters of earthquakes with magnitudes greater than 5.5 between 1984 and 2002. As for the synthetic data tests, we require that each event have at least five differential times for *P* or *S* variations and that each 3-month time interval include more than 10 events for the robust mean calcula-

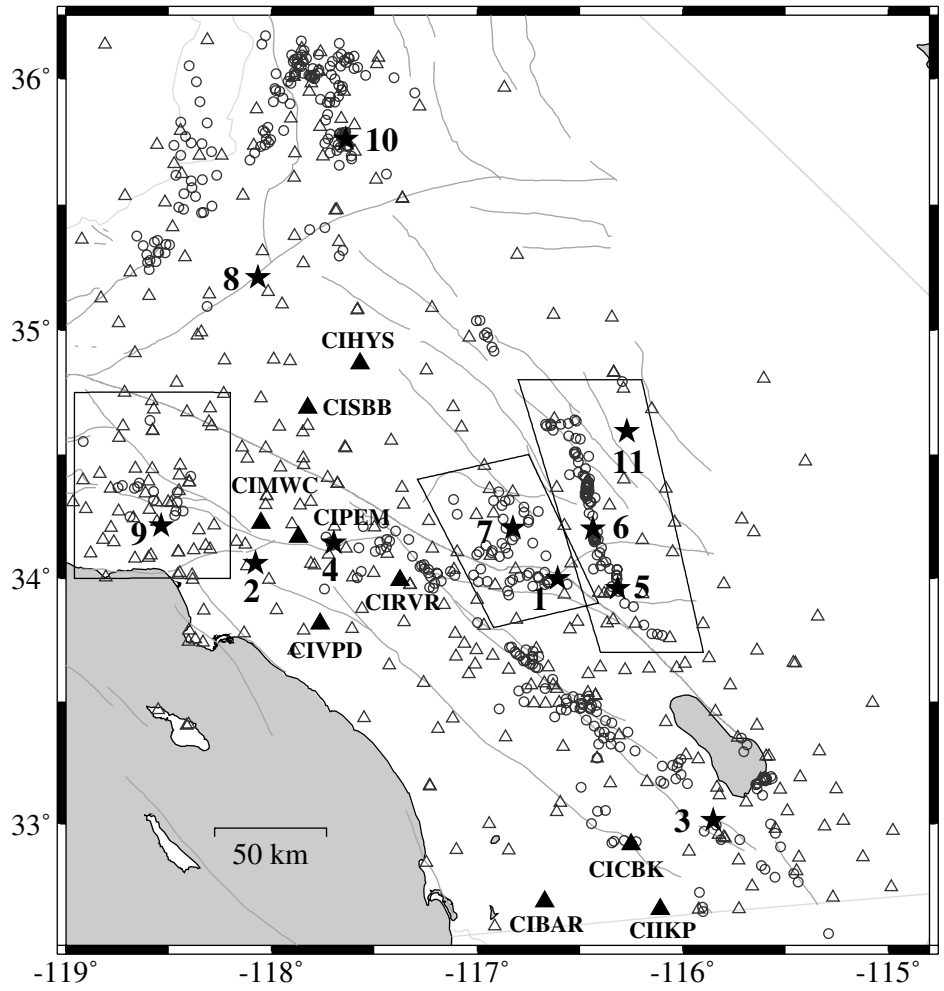

Figure 4. Locations of the event clusters and stations in our study. The triangles are the stations and the circles are the similar event clusters. The filled triangles are the nine stations with significant offsets in station corrections in our study with the station names next to them. The stars show some large mainshocks in our study area: 1, North Palm Springs (1986); 2, Whitter Narrows (1987); 3, Superstition Hills (1987); 4, Upland (1990); 5, Joshua Tree (1992); 6, Landers (1992); 7, Big Bear (1992); 8, Mojave (1992); 9, Northridge (1994); 10, Ridgecrest (1995); and 11, Hector Mine (1999). The boxes enclose the subregions for the temporal velocity variation study described in a later section.

tion. The bulk of the resulting time-varying station-term estimates for the 166 stations have what appears to be largely random scatter, but nine stations have obvious offsets in their station-term time series.

Anomalous Station-Term Offsets

The station-term estimates for these nine stations are plotted in Figure 5, and their apparent offset times are listed in Table 1. The offsets range from about 20 to 70 msec and occurred at distinctly different times, although the exact occurrence time of each time offset is limited by our 3-month averaging interval. The *P* and *S* timing changes are about the same at each station. This suggests that the source of the timing offsets is instrumental rather than a change in the Earth's seismic properties because it is not likely that changes in seismic velocities would produce identical time offsets for both *P* and *S*.

We checked SCSN station records between 1984 and 2002 and found that some of these stations indeed experienced instrument changes during our study period. The change consisted of replacing an old Caltech or Develco Voltage Controlled Oscillator and filters with U.S. Geological Survey (USGS) J5 Amp/VCO filters. The new equipment at these sites gave them the same response as the other short-period stations. The timing difference may be due to slightly different passband or phase response in the filters. We list the times for these hardware changes in Table 1. For stations CIBAR, CIMWC, CIRVR, CISBB, and CIVPD, the offsets in the station corrections happened at the time of the equipment changes. For stations CICBK, CIHYS, and CIPEM, there is no associated equipment change information available from the SCSN, and they seem to have gradual

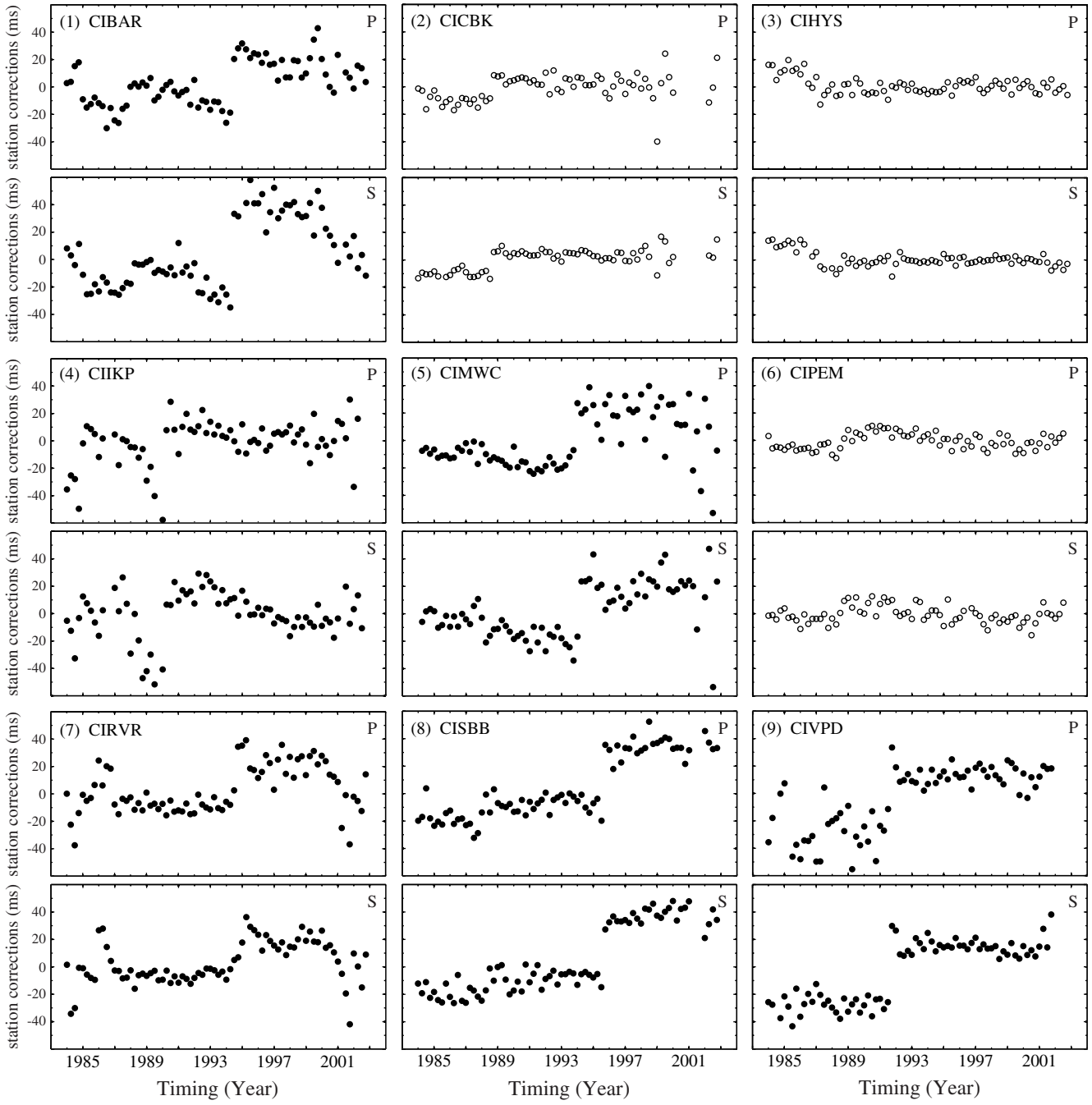

Figure 5. Time-varying station-term estimates for nine stations that have sharp timing offsets. Filled circles show station terms at the stations where the equipment changes are reported. No reported equipment changes correspond to the station offsets shown by open circles at the other three stations.

changes in station corrections, which makes the timing of the offsets hard to estimate. However, due to the fact that the variations in *P* and *S* are almost equal, it seems likely that these variations may also be caused by instrumental effects. It is interesting that for station CIIKP the equipment changes occurred in 1995 while a timing offset is observed in 1990. Although we do observe a slight increase in station corrections for *P* in 1995, they are not as dramatic as those in 1990, so there might be some unreported equipment changes in 1990.

Random Station-Term Variations

Except for the nine stations presented in the last section, most of the other stations in our study seem to have largely random station-term signals. Figure 6 shows the station cor-

Table 1
Stations with Significant Timing Offsets

Station Name	Station Location		Number of Clusters	Δt_p (msec)	Δt_s (msec)	$\Delta t_s/\Delta t_p$	Offset Timing (mm/yyyy)	Equipment Change Timing (mm/dd/yyyy)
	Latitude (°)	Longitude (°)						
CIBAR	32.68005	−116.67215	96	52	70	1.35	01/1994–09/1994	08/1994
CICBK	32.91580	−116.25226	115	17	18	1	04/1988–12/1988	—
CIHYS	34.86532	−117.56975	171	−26	−23	0.9	—	—
CIIKP	32.65012	−116.10948	64	70	65	0.9	01/1990–06/1990	11/02/1995
CIMWC	34.22368	−118.05287	79	39	44	1	07/1993–03/1994	09/20/1993
CIPEM	34.16689	−117.87009	95	21	20	1	—	—
CIRVR	33.99351	−117.37546	128	42	30	0.7	04/1994–12/1994	08/04/1994
CISBB	34.68817	−117.82501	84	42	39	0.9	07/1995–12/1995	10/30/1995
CIVPD	33.81596	−117.76338	85	37	37	1	07/1991–12/1991	10/17/1991

rection variations for nine randomly selected stations. Most of the station corrections for these stations are less than 10 msec. There are hints at some gradual variations, such as in stations CIELS, CIJNH, and CISS2, and station CIDTP has a small drop in 1988. It is possible that these signals are caused by seismic velocity changes beneath the stations, but they are close to the background noise level. It is difficult to be sure that they are not due to some unknown instrumental effect or artifact in our processing.

Temporal Seismic Velocity Variations?

Our results place overall limits of about 10 msec on *P* and *S* travel-time variations caused by seismic velocity changes beneath individual SCSN stations over our observing period. However, it is possible that larger travel-time anomalies are caused by localized velocity perturbations at depth. If only selected rays from each station sample a perturbed region, then the anomaly would not necessarily appear in plots of average station term versus time because its effects could be greatly diluted by averaging with the residuals from the nonanomalous paths. One way to test for this possibility would be to perform time-dependent tomography to invert for possible velocity anomalies in time and space. However, such an analysis would need to be performed very carefully because of the limited ray coverage, the time evolution of the active clusters, and the substantial scatter in the individual differential time residuals. As an alternative, we experimented with various ways to plot our results to see if we could identify any clear anomalies. First, we tried plotting the most anomalous residuals along individual ray paths at 1-yr intervals. These results (not shown here) were difficult to interpret because of the many overlapping ray paths and exhibited no consistent patterns. Next we computed the robust means of the *P*-wave station corrections in a 15° azimuth bin for each station. Plotting the results at 6-month intervals again showed no robust anomalies that appeared on multiple stations. However, we did notice increased residuals for stations in the Northridge and Imperial Valley regions. This can also be seen in a summary plot of the station residuals spanning the entire time period (Fig. 7), where the source–receiver azimuth is indicated in the pie charts at each station and the wedge color indicates the value of the mean station correction, with blue for less than −20 msec, red for more than 20 msec, and green to orange for values between −20 and 20 msec. The results show azimuthal variations in the residuals at a number of stations, but it is difficult to identify specific anomalies causing these features.

We were able to obtain clearer results when we examined the residuals at the earthquake cluster locations rather than the station locations. Because the travel-time residuals for individual events are always zero (as any nonzero residual is absorbed into a change in the origin time), we examined the standard deviation of the residuals versus time, plotted at the event locations. Increased scatter (as measured by the standard deviation) in the residuals might be expected if there were azimuthally dependent velocity changes in the vicinity of the events. We examined plots of the event residual standard deviations at 3- and 6-month intervals and found considerable variation among the individual events. The largest and most robust anomalies are increased residual scatter immediately following the *M* 7.3 Landers and *M* 6.7 Northridge earthquakes for similar event clusters within their aftershock sequences. The increased scatter does not appear for clusters elsewhere in southern California during the same time period. The observed scatter is greatest in the 3-month interval following the mainshocks and then lessens with time.

In Figure 8, we show the standard deviations of residuals for each event in 3-month intervals in the Landers and Big Bear regions from March 1992 to March 1993, from 3 months before to 9 months after the mainshocks. Large values of more than ±20 msec are shown by the black dots, and the percentage of these large values decreases with the time following the mainshocks. The first 3-month interval shows mostly aftershocks from the 1992 *M* 6.1 Joshua Tree earthquake, during which time 14% of the residuals exceed ±20 msec. The fraction of anomalous residuals increases to 18% immediately after the Landers and Big Bear earthquakes and then gradually drops to 13% after 9 months. Similar plots for the Northridge region are shown in Figure 9 at 3-month intervals during the year following the mainshock.

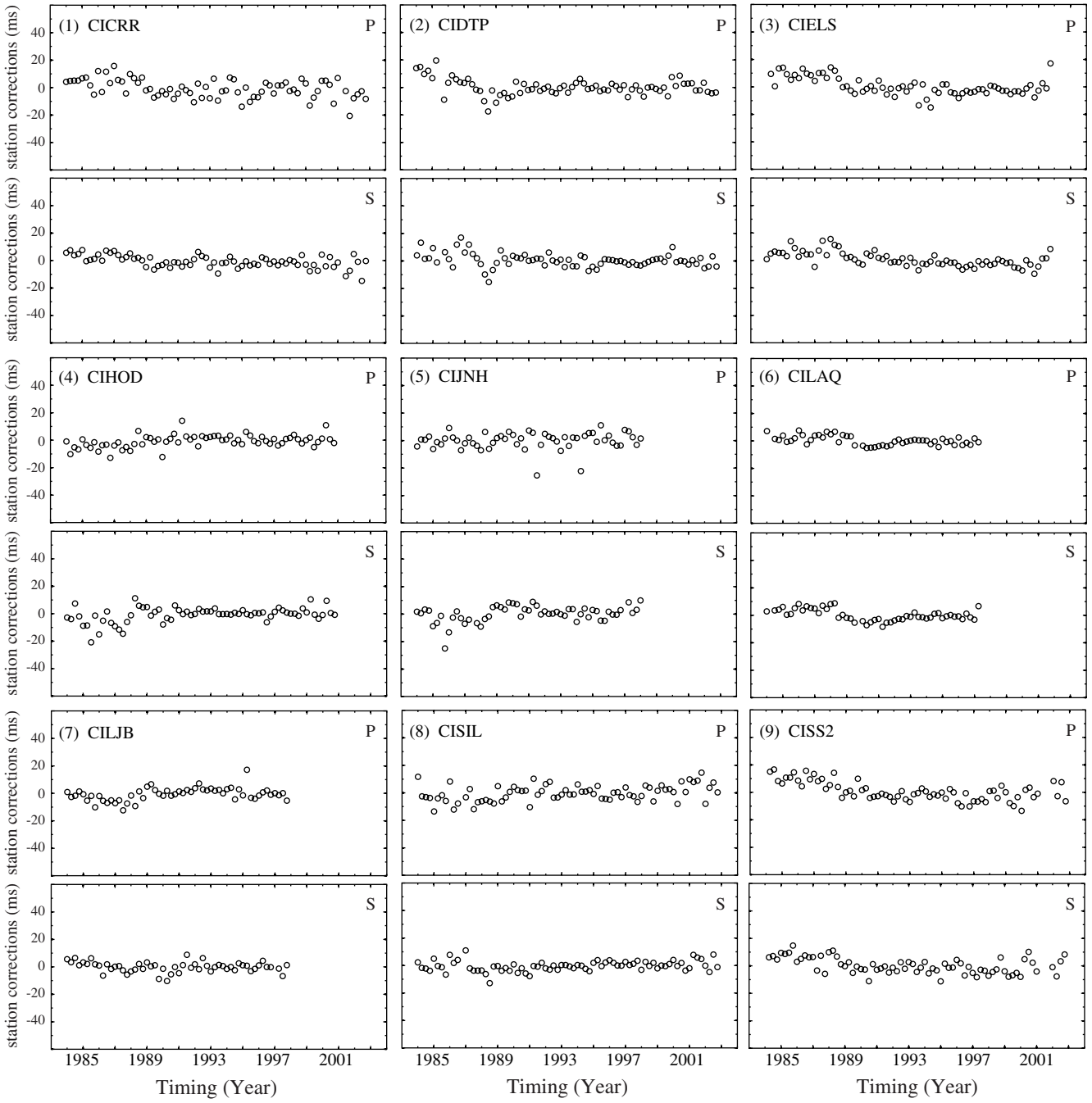

Figure 6. *P*- and *S*-wave station-term estimates for nine selected stations.

The percentage of large residuals gradually drops from 37% in the 3 months immediately after the mainshock to about 16% a year later. It would be interesting to look for a similar pattern following the 1999 *M* 7.1 Hector Mine earthquake, but unfortunately our selection criteria do not include any similar event clusters within the Hector Mine aftershock sequence. We observe slightly increased residual scatter across southern California that begins about a year before the Hector Mine earthquake and lasts about 3 yr. However, we observe no spatial correlation between this anomaly and the location of the Hector Mine mainshock. Thus, we think this anomaly is most likely caused by some change in the network, such as the installation of the broadband TriNet stations near this time (Hauksson *et al.*, 2001), that we have not fully corrected for in our analysis.

In Figure 10, we show the number of differential time residuals and percentages of large station corrections relative to the total number of corrections in different areas, plotted as a function of time to compare with the mainshock origin times (shown as the vertical lines). In order to obtain robust esti-

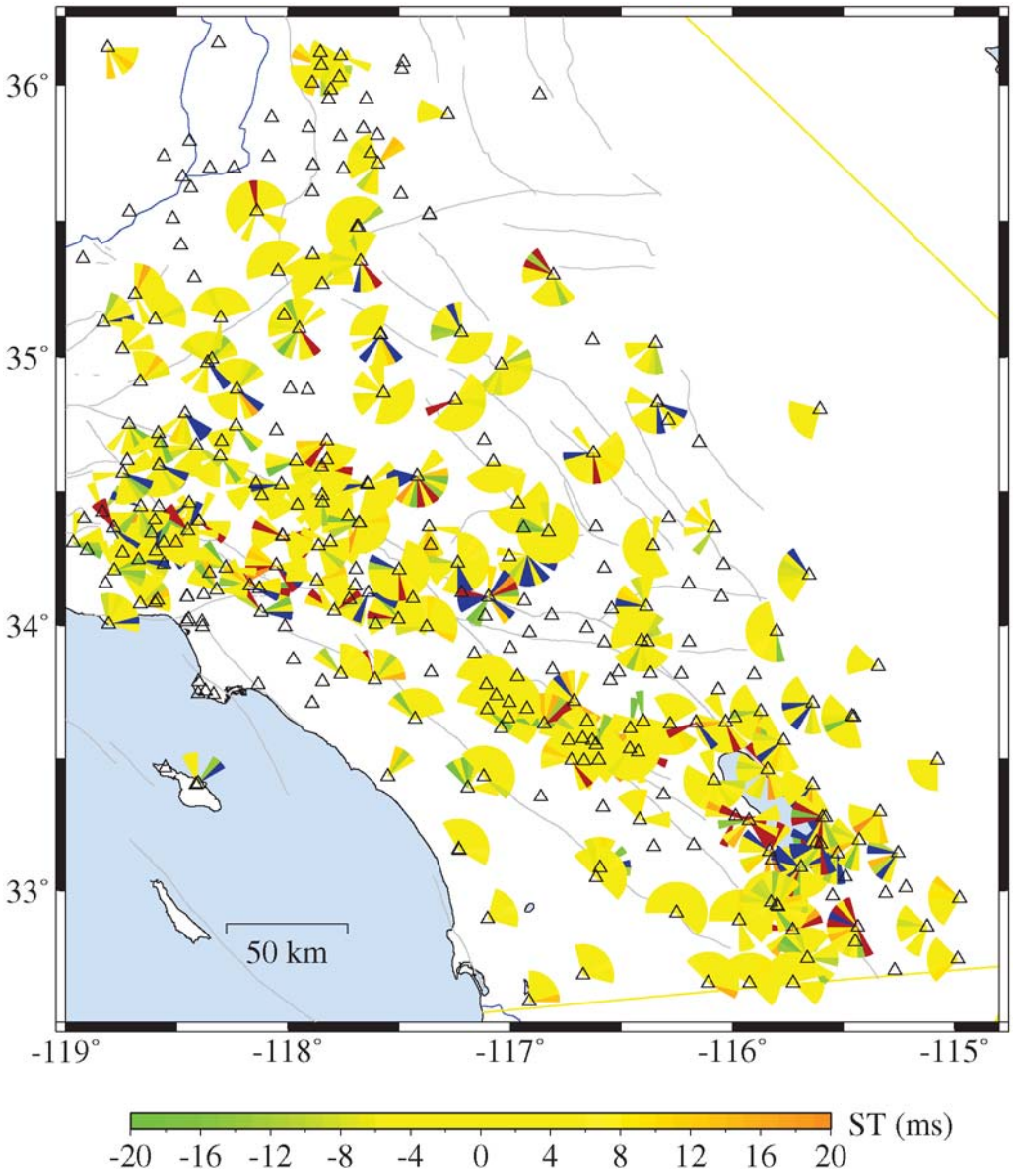

Figure 7. *P*-wave station correction average values in 15° azimuth bins for each station colored by their values, with blue for less than −20 msec and red for more than 20 msec.

mates, we plot the points only if there are more than 20 residuals in that period. We examined three regions in particular detail, as defined by the boxes plotted in Figure 4 around Northridge, Big Bear, and Landers and Hector Mine. Results for event clusters in these subareas are shown in Figure 10b, c,d, with the anomalous residual percentages relative only to the numbers in each region. For the Landers and Hector Mine box and the Northridge box, there were few earthquakes before the mainshocks, so we do not show any points at these earlier times. The largest number of residuals occurs immediately following each mainshock due to aftershock activity and then decays as the aftershocks diminish. In Figure 10a, there is a huge increase in the number of differential time residuals in 1992, corresponding to the 1992 Joshua Tree, Big Bear, Landers, and Mojave sequences. Notice that the data count plotted in the histograms in the top parts of Figure 10 is not necessarily exactly proportional to total seismic activity because it depends upon the number of similar event clusters observed in our catalog.

The bottom parts of Figure 10 show the percentage of station-term residuals greater than 20 msec (red curves) or less than −20 msec (blue curves). The mainshocks are associated with a notable increase in anomalously large residuals, especially for the positive values. The most significant anomaly peaks are observed in the Landers and Hector Mine area and in the Northridge area in Figure 10b,d. For the Big Bear area, it is more complicated because of the ongoing seismic activity in this area, including the 1986 North Palm Springs and other earthquakes. The apparent slight precursory anomaly seen in Figure 10a,b before the 1992 Landers earthquake

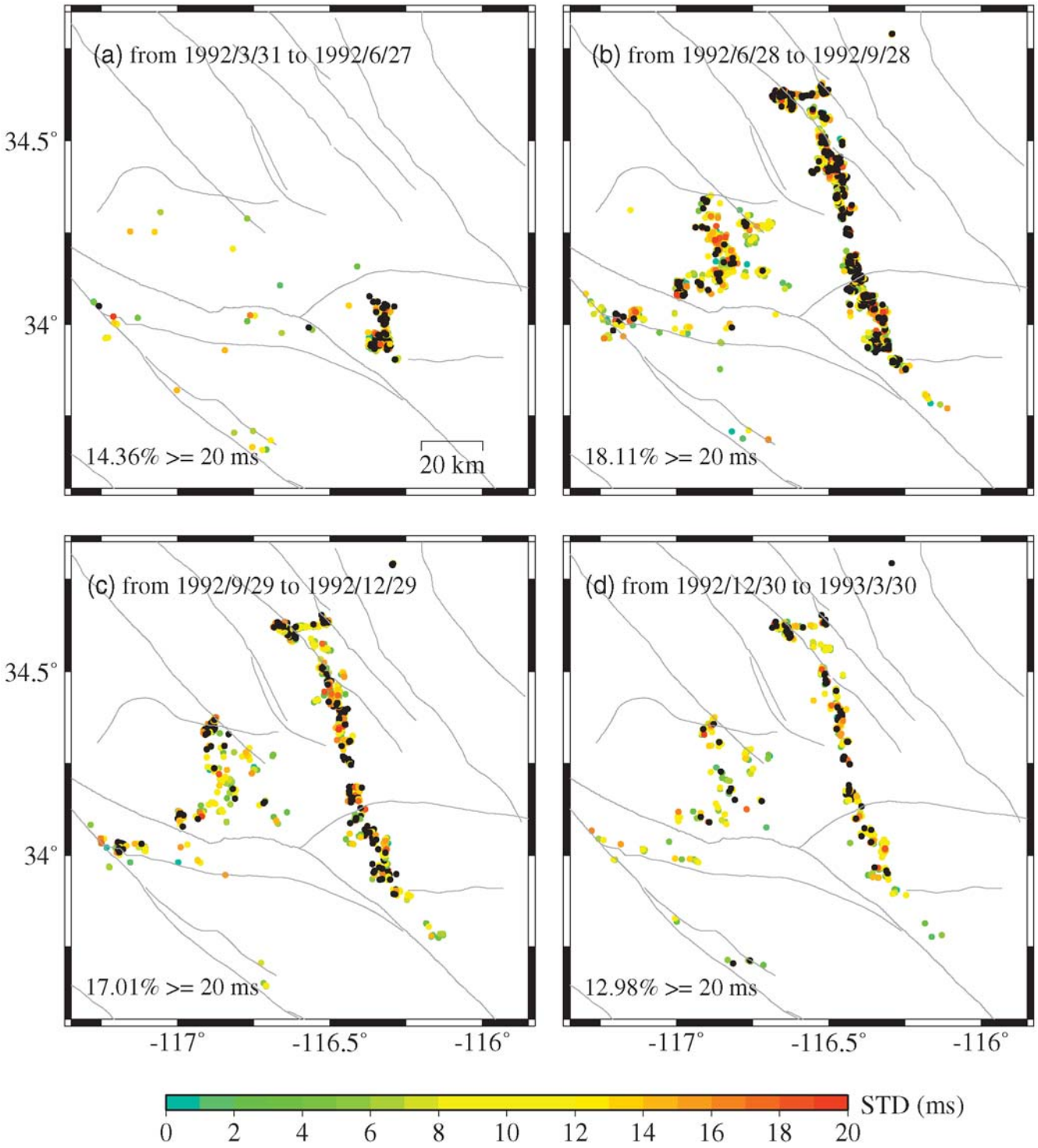

Figure 8. Event-specific residual standard deviations for the Landers and Big Bear regions. Gray lines denote surface traces of mapped faults. (a) 0–3 month activity before the 28 June 1992 Landers and Big Bear mainshocks. (b) 0–3 month activity after the mainshocks. (c) 3–6 month activity after the mainshocks. (d) 6–9 month activity after the mainshocks. Events are colored by the residual standard deviation values, with black for more than 20 msec.

is likely caused by the M_w 6.1 Joshua Tree earthquake 2 months earlier. There is an increase in the number of positive residuals within the Landers and Hector Mine box near the time of the 1999 Hector Mine earthquake. However, this is caused by a relatively small number of events within the Landers aftershock region because we do not have any similar event clusters within the Hector Mine aftershocks (note that Fig. 10b does not show increased numbers of events in 1999). As discussed previously, we do not think this anomaly is associated with the Hector Mine earthquake.

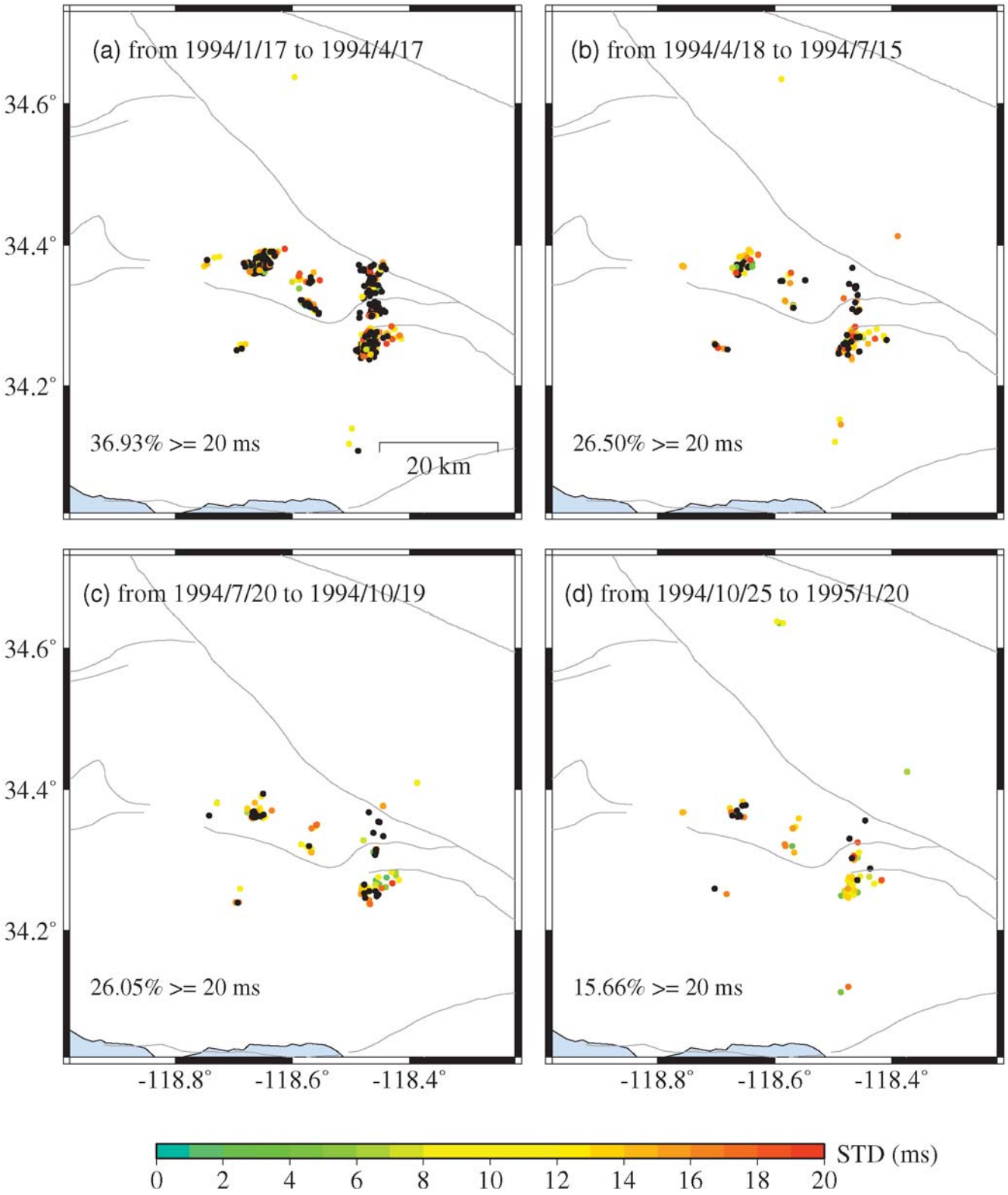

Figure 9. Event-specific residual standard deviations for the Northridge region. (a) 0–3 month activity after the 17 January 1994 Northridge mainshock. (b) 3–6 month activity after the mainshock. (c) 6–9 month activity after the mainshock. (d) 9–12 month activity after the mainshock. Events are colored by the residual standard deviation values, with black for more than 20 msec.

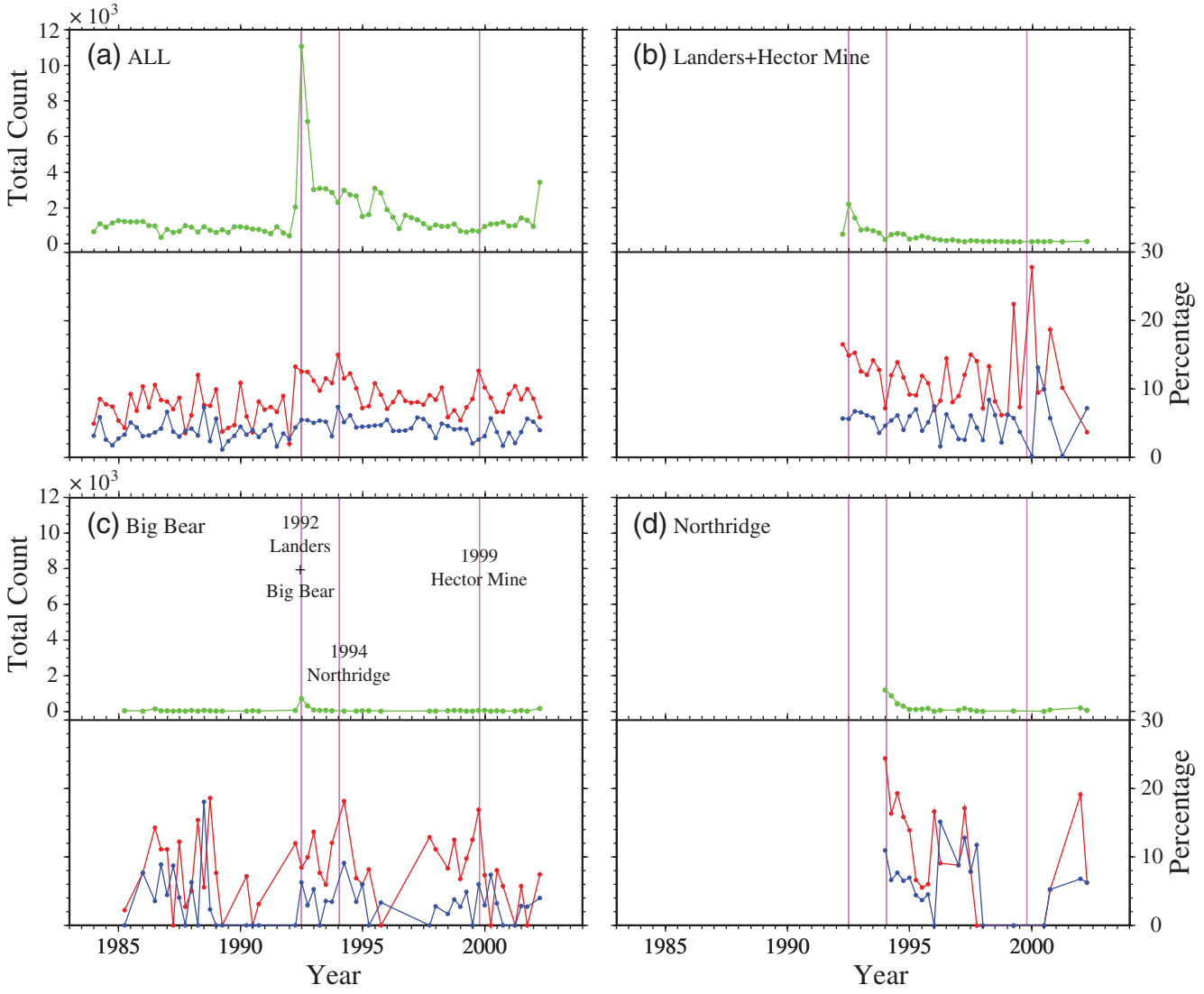

Figure 10. The number of individual cluster-to-station paths (top panels) and the fraction of *P*-wave travel-time residuals exceeding ±20 msec (bottom panels) for (a) our entire dataset, (b) a region around the 1992 Landers and 1999 Hector Mine earthquakes, (c) a region around the 1992 Big Bear earthquake, and (d) a region around the 1994 Northridge earthquake. The subregion boundaries are plotted in Figure 4 and include most of the aftershocks of these events. The red lines show the fraction of residuals larger than 20 msec, while the blue lines show the fraction of residuals less than −20 msec. For reference, the three vertical lines show the times of the 1992 Landers–Big Bear, 1994 Northridge, and 1999 Hector Mine earthquakes.

In our sign convention, positive station terms correspond to reduced velocities, if they are caused by velocity variations. Previous studies have identified temporal variations in seismic velocity, coda *Q*, and scattering properties of the crust associated with large earthquakes (Poupinet *et al.*, 1984; Ellsworth *et al.*, 1987; Got *et al.*, 1990; Ellsworth *et al.*, 1992; Haase *et al.*, 1995; Dodge and Beroza, 1997; Baisch and Bokelmann, 2001; Nakamura *et al.*, 2002; Rubinstein and Beroza, 2004; Peng and Ben-Zion, 2006; Sawazaki *et al.*, 2006; Li *et al.*, 2007). Our results agree with the common property of the reported velocity changes that a decrease in velocity often happens at the time of the earthquake, perhaps caused by the formation or opening of cracks, but that the amplitude of this anomaly generally decreases with time following the mainshock (i.e., the velocity increases), suggesting some kind of healing process. Gradual increases in velocity have also been reported following large earthquakes in fault-zone trapped waves observed following the Landers and Hector Mine earthquakes (Li *et al.*, 1998, 2003).

Note that our method would not be very sensitive to seismic velocity changes in the immediate vicinity of each similar event cluster. These changes would affect travel times along all of the ray paths from the cluster by roughly the same amount and would be compensated for by a change in the event origin times in our relocation procedure. The increase in the residuals must therefore result from nonuniform velocity changes among the paths and stations recording each cluster. A more detailed analysis of individual

aftershock sequences might be able to sort out these effects and produce maps of the estimated velocity changes following each mainshock, but it is not clear if the signal is coherent enough for the results to be very detailed.

Discussion

Unlike many parts of northern California (e.g., Rubin *et al.*, 1999; Waldhauser *et al.*, 1999; Waldhauser and Ellsworth, 2000), there are not many repeating earthquakes with identical waveforms in southern California. The event pairs in our study are not highly correlated with each other (i.e., they have average correlation coefficients above 0.6 rather than the 0.95 and higher correlations seen for repeating events). This leads to some degree of scatter in the differential times and their residuals following event relocation, although some scatter might also be due to the unaccounted for 3D heterogeneity comparable in scale to the 1–2 km size of the similar event clusters. We reduce the effects of this scatter by using robust misfit criteria throughout our analyses (so that the results are not biased by large errors in some of the cross-correlation times) and by examining the results in 3-month windows. The clearest signal in our time-dependent station terms are abrupt offsets of 20–70 msec observed at nine stations, which are likely due to equipment changes. The variations observed at the other stations are no more than about ± 10 msec. In some cases, there appear to be gradual changes in station terms, which might be caused by small temporal velocity variations beneath the receivers, although these are close to the resolution limit of our technique. In principle, removing the time-dependent station terms could help us improve relative event locations (as was done by Rubin [2002] for some northern California clusters), but we do not attempt this here.

We can convert the arrival-time residual along each cluster-station ray path into apparent velocity variations based on the 1D velocity model used in the differential time relocation. The standard deviation of the resulting *P*-velocity changes is 0.18%. This agrees with the results in Haase *et al.* (1995) on the temporal velocity variations near the Anza, California, region based on a 9-yr period dataset. Both studies use differential times for similar event pairs from waveform cross correlation. Haase *et al.* (1995) selected event pairs with correlation coefficients greater than 0.9 and concluded that it is unlikely that there is a systematic temporal change in seismic velocity greater than 0.2% due to a localized accumulation of stress within their study region. Our study extends this null result to most of southern California over a longer time period (from 1984 to 2002). Although our spatial and temporal resolution is limited to some extent by our ray coverage and our 3-month averaging interval, our results suggest that any long-lasting seismic velocity perturbations over significant portions of the southern California crust must be less than about $\pm 0.2\%$. In particular, we observe no precursory variations in seismic velocity prior to large earthquakes that might be caused by accelerated stress or strain rates in the months and years prior to rupture.

Data and Resources

All data used in this article came from published sources listed in the references. Plots were made using the public domain Generic Mapping Tool (GMT) software (Wessel and Smith, 1991) and Matlab.

Acknowledgments

We thank Jeanne Hardebeck, David Schaff, and an anonymous reviewer for their detailed and constructive reviews. Funding for this research was provided by the National Earthquake Hazards Reduction Program (NEHRP) and USGS Grant Number 03HQPA0001. This research was also supported by the Southern California Earthquake Center (SCEC), which is funded by National Science Foundation (NSF) Cooperative Agreement Number EAR-0106924 and USGS Cooperative Agreement Number 02HQAG0008. The SCEC contribution number for this article is 1123.

References

Astiz, L., and P. M. Shearer (2000). Earthquake locations in the inner continental borderland, offshore southern California, *Bull. Seismol. Soc. Am.* **90,** 425–449.

Astiz, L., P. M. Shearer, and D. C. Agnew (2000). Precise relocations and stress change calculations for the Upland earthquake sequence in southern California, *J. Geophys. Res.* **105,** 2937–2953.

Baisch, S., and G. H. R. Bokelmann (2001). Seismic waveform attributes before and after the Loma Prieta earthquake: scattering change near the earthquake and temporal recovery, *J. Geophys. Res.* **106,** 16,323–16,337.

Dodge, D. A., and G. C. Beroza (1997). Source array analysis of coda waves near the 1989 Loma Prieta California, mainshock: implications for the mechanism of coseismic velocity changes, *J. Geophys. Res.* **102,** 24,437–24,458.

Dodge, D. A., G. C. Beroza, and W. L. Ellsworth (1995). Foreshock sequence of the 1992 Landers, California, earthquake and its implications for earthquake nucleation, *J. Geophys. Res.* **100,** 9865–9880.

Ellsworth, W. L., A. T. Cole, G. C. Beroza, and M. C. Verwoerd (1992). Changes in crustal wave velocity associated with the 1989 Loma Prieta, California earthquake (Abstract S21D-1), *EOS Trans. AGU* **73,** S21D-1.

Ellsworth, W. L., L. D. Dietz, J. Fréchet, and G. Poupinet (1987). Preliminary results on the temporal stability of coda waves in central California from high-precision measurements of characteristic earthquakes, *U.S. Geol. Surv. Open-File Rept. 87-591*, 440–460.

Gillard, D., A. M. Rubin, and P. Okubo (1996). Highly concentrated seismicity caused by deformation of Kilauea's deep magma system, *Nature* **384,** 343–346.

Got, J.-L., J. Fréchet, and F. W. Klein (1994). Deep fault plane geometry inferred from multiplet relative relocation beneath the south flank of Kilauea, *J. Geophys. Res.* **99,** 15,375–15,386.

Got, J. L., G. Poupinet, and J. Fréchet (1990). Changes in source and site effects compared to coda Q1 temporal variations using microearthquakes doublets in California, *Pure Appl. Geophys.* **134,** 195–228.

Haase, J. S., P. M. Shearer, and R. C. Aster (1995). Constraints on temporal variations in velocity near Anza, California, from analysis of similar event pairs, *Bull. Seismol. Soc. Am.* **85,** 194–206.

Hauksson, E., and P. Shearer (2005). Southern California hypocenter relocation with waveform cross-correlation, part I: Results using the double-difference method, *Bull. Seismol. Soc. Am.* **95,** 896–903.

Hauksson, E., P. Small, K. Hafner, R. Busby, R. Clayton, J. Goltz, T. Heaton, K. Hutton, H. Kanamori, J. Polet, D. Given, L. M. Jones, and D. Wald

(2001). Southern California Seismic Network: Caltech/USGS Element of Trinet 1997–2001, *Seism. Res. Lett.* **72,** 690–704.

Li, Y.-G., P. Chen, E. S. Cochran, and J. E. Vidale (2007). Seismic velocity variations on the San Andreas fault caused by the 2004 *M* 6 Parkfield earthquake and their implications, *Earth Planets Space* **59,** 21–31.

Li, Y.-G., J. E. Vidale, K. Aki, F. Xu, and T. Burdette (1998). Evidence of shallow fault zone strengthening after the 1992 *M* 7.5 Landers, California, earthquake, *Science* **279,** 217–219.

Li, Y.-G., J. E. Vidale, S. M. Day, D. D. Oglesby, and E. S. Cochran (2003). Postseismic fault healing on the rupture zone of the 1999 *M* 7.1 Hector Mine, California, earthquake, *Bull. Seismol. Soc. Am.* **93,** 854–869.

Lin, G., and P. M. Shearer (2007). Estimating local Vp/Vs ratios within similar earthquake clusters, *Bull. Seismol. Soc. Am.* **97,** 379–388.

Lin, G., P. M. Shearer, and E. Hauksson (2007). Applying a three-dimensional velocity model, waveform cross correlation, and cluster analysis to locate southern California seismicity from 1981 to 2005, *J. Geophys. Res.* **112,** B12309, doi 10.1029/2007JB004986.

Nadeau, R. M., W. Foxall, and T. V. McEvilly (1995). Clustering and periodic recurrence of microearthquakes on the San Andreas fault at Parkfield, California, *Science* **267,** 503–507.

Nakamura, Y. (1978). A_1 moonquakes: source distribution and mechanism, in *Proc. of the 9th Lunar Planet. Sci. Conf.*, 3589–3607.

Nakamura, A., A. Hasegawa, N. Hirata, T. Iwasaki, and H. Hamaguchi (2002). Temporal variations of seismic wave velocity associated with 1998 *M* 6.1 Shizukuishi earthquake, *Pure Appl. Geophys.* **159,** 1183–1204.

Peng, Z., and Y. Ben-Zion (2006). Temporal changes of shallow seismic velocity around the Karadere-Duzce branch of the north Anatolian fault and strong ground motion, *Pure Appl. Geophys.* **163,** 567–600.

Poupinet, G., W. L. Ellsworth, and J. Frechet (1984). Monitoring velocity variations in the crust using earthquake doublets: an application to the Calaveras fault, California, *J. Geophys. Res.* **89,** 5719–5732.

Rowe, C., C. Thurber, and R. White (2004). Dome growth behavior at Soufriere Hills Volcano, Montserrat, revealed by relocation of volcanic event swarms, 1995–1996, *J. Volcanol. Geotherm. Res.* **134,** 199–221.

Rubin, A. M. (2002). Using repeating earthquakes to correct high-precision earthquake catalogs for time-dependent station delays, *Bull. Seismol. Soc. Am.* **92,** 1647–1659.

Rubin, A. M., D. Gillard, and J.-L. Got (1999). Streaks of microearthquakes along creeping faults, *Nature* **400,** 635–641.

Rubinstein, J. L., and G. C. Beroza (2004). Evidence for widespread nonlinear strong ground motion in the M_w 6.9 Loma Prieta earthquake, *Bull. Seismol. Soc. Am.* **94,** 1595–1608.

Sawazaki, K., H. Sato, H. Nakahara, and T. Nishimura (2006). Temporal change in site response caused by earthquake strong motion as revealed from coda spectral ratio measurement, *Geophys. Res. Lett.* **33,** L21303, doi 10.1029/2006GL027938.

Schaff, D. P., and F. Waldhauser (2005). Waveform cross-correlation-based differential travel-time measurements at the Northern California Seismic Network, *Bull. Seismol. Soc. Am.* **95,** 2446–2461.

Shearer, P. M. (1997). Improving local earthquake locations using the L1 norm and waveform cross correlation: application to the Whittier Narrows, California, aftershock sequence, *J. Geophys. Res.* **102,** 8269–8283.

Shearer, P. M. (1998). Evidence from a cluster of small earthquakes for a fault at 18 km depth beneath Oak Ridge, southern California, *Bull. Seismol. Soc. Am.* **88,** 1327–1336.

Shearer, P. M. (2002). Parallel fault strands at 9-km depth resolved on the Imperial fault, southern California, *Geophys. Res. Lett.* **29,** 1674, doi 10.1029/2002GL015302.

Shearer, P. M., J. L. Hardebeck, L. Astiz, and K. B. Richards-Dinger (2003). Analysis of similar event clusters in aftershocks of the 1994 Northridge, California, earthquake, *J. Geophys. Res.* **108,** no. B1, 2035, doi 10.1029/2001JB000685.

Shearer, P. M., E. Hauksson, and G. Lin (2005). Southern California hypocenter relocation with waveform cross-correlation, part II: Results using source-specific station terms and cluster analysis, *Bull. Seismol. Soc. Am.* **95,** 904–915.

Waldhauser, F., and W. L. Ellsworth (2000). A double-difference earthquake location algorithm: method and application to the Northern Hayward fault, California, *Bull. Seismol. Soc. Am.* **90,** 1353–1368.

Waldhauser, F., W. L. Ellsworth, and A. Cole (1999). Slip-parallel seismic lineations on the northern Hayward fault, California, *Geophys. Res. Lett.* **26,** 3525–3528.

Wessel, P., and W. H. F. Smith (1991). Free software helps map and display data, *EOS Trans. AGU* **72,** 441.

Institute of Geophysics and Planetary Physics,
Scripps Institution of Oceanography
University of California, San Diego
La Jolla, California 92093-0225
(G.L., P.M.S.)

Seismological Laboratory
MS 252-21
California Institute of Technology
Pasadena, California 91125
(E.H.)

Manuscript received 1 October 2007